Pulse growth dynamics in laser mode locking

Mark Popov and Omri Gat

Racah Institute of Physics, The Hebrew University, Jerusalem 9190401, Israel

We analyze theoretically and numerically the nonlinear process of pulse formation in mode-locked lasers, starting from a perturbation of a continuous wave. Focusing on weak-to-moderate dispersion systems, we show that pulse growth is initially slow, dominated by a cascade of energy from low to high axial modes, followed by fast strongly nonlinear growth, and finally relaxation to the stable pulse wave form. The pulse grows initially by condensing a fixed amount of energy into a decreasing time interval, with peak power growing toward a finite-time singularity that is checked when the gain bandwidth is saturated by the pulse.

Introduction. Passive mode locking is essential for the creation of ultrashort pulses, and as such has long been the subject of intense study [1,2]. The complex evolution of the optical wave form in passive mode-locked lasers (PMLs) is an extended nonlinear dynamical system. While the stationary pulse states of PMLs are well understood [3,4], a systematic theory of the rich variety of transient and unsteady states of PMLs is still lacking.

Here, we focus on a transient process of particular importance—the buildup of an ultrashort pulse from an initial weak narrow-band quasicontinuous wave. The pulse growth dynamics has been studied in several papers, starting in the 1990's [5–13], where the main goal was to study the question of self-starting; this question was later answered by a statistical mechanics analysis of the laser, where mode locking is a thermodynamic phase transition [14–18].

The early studies focused on the initial stages of the growth process, and experimental data on the later evolution of the wave form have been limited. More recently, there has been a resurgence of interest in the subject with the advent of experimental techniques allowing for real-time tracking of the evolving optical wave form [19–22].

On the other hand, the theoretical understanding of the pulse growth process is rudimentary: From a dynamical systems perspective [23], the wave-form trajectory is a heteroclinic orbit connecting an unstable fixed point, continuous wave (cw), and a stable pulse fixed point. The fixed points, that are stationary solutions of the governing equations, are well studied, and so is the linearized dynamics very close to them. However, the bulk of the evolution dynamics is nonlinear, and exhibits considerable complexity [19–22].

We tackle this problem numerically and theoretically, in an approach based on the Haus mode-locking model with slow gain and fast saturable absorption; systems that fall into this category include the common cases of fiber lasers mode locked with nonlinear polarization rotation, and Kerr-lens mode-locked Ti:sapphire lasers [1]. The first key conclusion is that the nature of pulse growth depends critically on the strength of the dispersive effects—group-velocity dispersion and Kerr nonlinearity—relative to the gain and loss. When the dispersive effects are weak or comparable to the gain and

loss terms, the peak power of the pulse grows monotonically, and the pulse width decreases monotonically, as the wave form evolves from cw to pulse, and the growth dynamics is reproducible; when dispersive effects are strong, on the other hand, the wave form evolves in an oscillatory and chaotic manner, and the pulse generation is a stochastic event. The strong dispersion regime is typical for ultrashort pulse lasers [21].

Here, we study the simpler weak-to-moderate dispersion regime, which is relevant to picosecond pulse lasers. We show that although the final stages of pulse formation occur on a fast nonlinear time scale of order μs, it is preceded by a slow growth process that is one to two orders of magnitudes slower. Moreover, whereas the final fast growth is strongly nonlinear, the initial slow dynamics is governed by a small parameter, the ratio of the spectral width to the final bandwidth.

We develop a weakly nonlinear theory for the slow growth process, showing that pulse buildup progresses through a cascade of power from lower to higher axial modes, driven by the absorptive and Kerr nonlinearities. We derive explicit recursive expressions for the mode amplitudes as series of growing exponentials, whose radius of convergence marks the transition to strongly nonlinear growth.

A principal result is that the slow process itself takes place in two stages. In the early stage, the bandwidth of the pulse is so small that gain filtering and dispersion are negligible; it leads to a *constant-power, form-invariant* pulse growth and narrowing toward a finite-time singularity. The singularity is averted by the gain response profile and dispersion, whose importance increases with the growing pulse bandwidth, causing the pulse shape to deform. The evolution of the pulse shape is fully described by the weakly nonlinear theory, and cannot be captured by reduced dynamical models of a small number of pulse parameters [24–26]. These theoretical predictions are compared with direct numerical simulations of the model, and shown to agree for several choices of model parameters in Figs. 1–3.

When the pulse peak power reaches 90% of its final value, the pulse shape is close enough to its final form that its dynamics is well approximated by relaxation of the normal modes of perturbation of the mode-locked state. In the cases
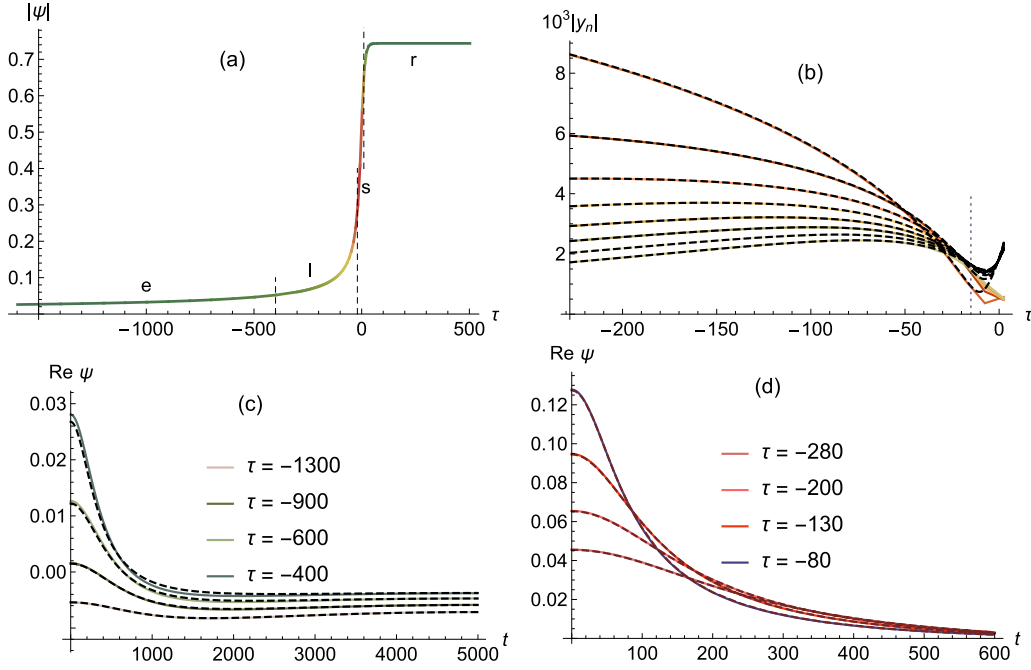
FIG. 1. Simulation results (solid curves) and corresponding theoretical calculation (dashed curves), reported in terms of natural units defined in the main text, for the pulse formation process with normalized dispersion $\beta = -1.5$, Kerr $\gamma = 0.6$, gain parameter $k = 2.7$, and chirp exponent $c = 1.58$. (a) The numerically calculated peak amplitude $|\psi(0,\tau)|$ as a function of the slow time τ. The growth stages marked on the graph are early weakly nonlinear (e), late weakly nonlinear (l), strongly nonlinear (s), and relaxation (r). The origin of τ is defined as the time where the pulse amplitude reaches one half of its final value. (b) The eight leading Fourier amplitudes $|y_n|$, $n = 0, 1, \ldots, 7$ ordered from top to bottom on the left, as a function of slow time τ (y_0 includes cw term.) Solid colored (grey) curves show simulation results, with higher modes in cooler colors, and dashed black curves show results of weakly nonlinear theory. The thin vertical dashed line marks the end of the validity domain of the weakly nonlinear expansion. (c), (d) Snapshots of Re $\psi(t,\tau)$, the real part of the wave form in simulation [solid colored (grey) curves] and theory (dashed black curves) as a function of fast time t for several values of τ in the (c) early and (d) late weakly nonlinear growth stage; later τ values correspond to stronger and narrower pulse wave forms. Note different scales between the two panels.

studied here, the dominant, least stable mode is a discrete mode, associated with amplitude perturbations [23,27,28]. It leads to exponential convergence toward the final pulse shape.

Laser model, steady states, and linear stability. We model the laser wave-form dynamics with the Haus master mode-locking equation,

$$
\frac{\partial \psi}{\partial \tau} = \left[\frac{g_u}{1 + P[\psi]/P_s} \left(1 - \frac{1}{\omega_g^2} \frac{\partial^2}{\partial t^2} \right) - l - i\beta_2 \frac{\partial^2}{\partial t^2} + (\gamma_s + i\gamma_k)|\psi|^2 \right]\psi,
\tag{1}
$$

in which ψ is the slowly varying electric field envelope depending on the fast and slow time coordinates t and τ (respectively), and g_u, l, P_s, ω_g, β_2, γ_s, and γ_k are the small signal gain and loss coefficients, gain saturation power, gain bandwidth, group-velocity dispersion, fast absorber saturability, and Kerr coefficient, respectively. The gain recovery time is assumed to be much longer than the round-trip time τ_R, so that the saturated gain depends only on the total power $P[\psi] = (1/\tau_R) \int_0^{\tau_R} |\psi|^2 dt$.

The simplest steady state of Eq. (1) is the dark state $\psi \equiv 0$, which is subject to the lasing instability, where the amplitude of an axial mode with frequency ω grows with rate $g_u(1 - \omega^2/\omega_g^2) - l$ (when this rate is positive) with a random phase. The growth of the lasing instability eventually leads to the cw

state. In the Haus model (1) the cw state is a wave form with a uniform amplitude a_c.

We now make the simplifying assumption, which usually holds in experiments, that the gain is deeply saturated, $P \gg P_s$, and then choose $1/\omega_g$, $1/l$, and $(l/\gamma_s)^{1/2}$ as units of t, τ, and ψ, respectively, so that the equation depends on four dimensionless combinations, $\beta = -\beta_2 \omega_g^2/l$, $\gamma = \gamma_k/\gamma_s$, $k = g_u P_s \gamma_s \tau_R \omega_g/l^2$, and $r = \tau_R \omega_g$, becoming

$$
\frac{\partial \psi}{\partial \tau} = \left[\frac{k}{\|\psi\|^2} \left(1 + \frac{\partial^2}{\partial t^2} \right) - 1 + i\beta \frac{\partial^2}{\partial t^2} + (1 + i\gamma)|\psi|^2 \right]\psi,
\tag{2}
$$

where $\|\psi\|^2 = \int_0^r |\psi|^2 dt$ (note that $\beta > 0$ corresponds to anomalous dispersion). r is the cavity round-trip time in the natural choice of units, and as such does not appear explicitly in (2); it effectively measures the number of active modes, so we let $r \gg 1$, leaving three order-1 parameters.

In this parametrization the cw solution is

$$
\psi_c(t,\tau) = a_c e^{i\Omega_c \tau}, \quad \frac{k}{a_c^2 r} = 1 - a_c^2, \quad \Omega_c = \gamma a_c^2,
\tag{3}
$$

which implies that $a_c \sim \sqrt{k/r} \ll 1$; here, Ω_c is the cw nonlinear frequency shift.
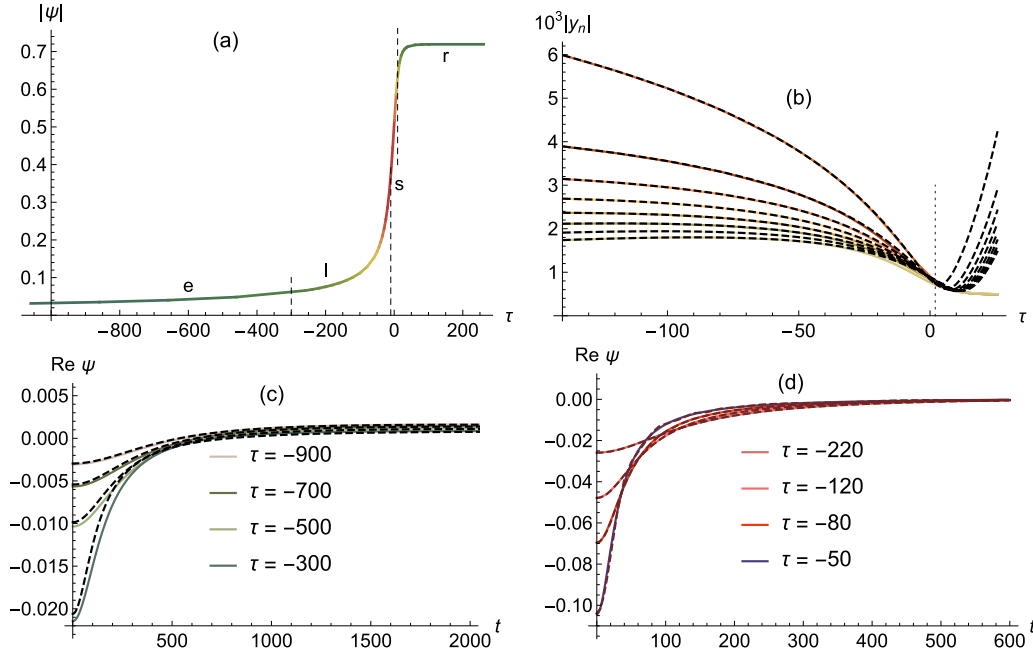
FIG. 2. Simulations and theory for pulse growth with $\beta = 1.0$, $\gamma = 0.2$, $k = 1.72$, $c = -0.53$. See Fig. 1 for panel descriptions.

To study perturbations to cw we write

$$\psi(t,\tau) = e^{i\Omega_c\tau}\sum_n [y_n(\tau) + \delta_{n,0}a_c]e^{i\omega_n t}, \quad \omega_n = 2\pi n/r,$$

(4)

where δ is the usual Kronecker delta; an infinitesimal perturbation to the cw evolves according to

$$y_0'(\tau) = \left[-1 + (1 + i\gamma)a_c^2\right](y_0 + y_0^*),$$

(5)

$$y_n'(\tau) = \left[(1 + i\gamma)a_c^2 - (1 + i\beta)\omega_n^2\right]y_n$$
$$+ (1 + i\gamma)a_c^2 y_n^*, \quad n \neq 0.$$

(6)

It follows that y_0 decays, while the growth rate of y_n, $n \neq 0$,

$$\lambda_n = a_c^2 - \omega_n^2 + \sqrt{a_c^4(1 + \gamma^2) - (\gamma a_c^2 - \beta\omega_n^2)^2},$$

(7)

is positive for sufficiently low modes since $\omega_n \ll r^{-1/2} \sim a_c$, making the cw modulationally unstable. We will assume that $\beta\gamma < 1$ and then $\lambda_1 = \lambda_{-1}$ are the largest growth rates.

We are interested in parameter values for which Eq. (2) has stable pulse steady-state solutions; these pulses are chirped-soliton shaped,

$$\psi_p(t,\tau) = a_p \operatorname{sech}(bt)^{1+ic}e^{i\Omega_p\tau}.$$

(8)

The pulse amplitude a_p, width $1/b$, chirp c, and nonlinear frequency shift Ω_p are determined by the physical parameters [1]. For fixed values of β, γ, and small enough k, there are two pulse solutions, of which the one with lower energy is stable [23].

Numerical calculations. We studied the formation of pulses by numerically solving Eq. (2) for several values of the (normalized) dispersion β and Kerr coefficient γ, yielding pulses with negative, zero, and positive chirp. For each choice of β and γ there is a maximal value of the gain parameter k that admits stable pulses, and the results shown here are for

k close to this maximum. We checked that the dynamics is weakly sensitive to changes in k.

In each of the simulations, the round-trip time was $r = 10^4$ natural units, which corresponds to a physical repetition rate of around 100 MHz, and the initial wave form was the cw solution perturbed along the most unstable mode with an amplitude of 10^{-8} natural units, corresponding to fluctuations of the order 10^{-7} W in the mode. The wave equation was solved with two methods, fourth-/fifth-order Runge-Kutta with a variable grid, and pseudospectral split step, with compatible results. Results reported here were obtained with the first method.

The simulations results are presented in Figs. 1–3, with Figs. 1(a), 2(a) and 3(a) showing the growth of the peak amplitude of the pulse, Figs. 1(b), 2(b) and 3(b) the evolution of the amplitudes of the first few axial modes, and Figs. 1(c), 2(c), 3(c) and 1(d), 2(d), and 3(d) the evolution of the real part of the waveform. Panels (b), (c), and (d) compare the simulation results with weakly nonlinear theory, showing very good agreement.

Mode energy cascade in weakly nonlinear pulse growth. For the weakly nonlinear analysis we assume that the y_n's are small but not infinitesimal, write Eq. (2) in terms of mode amplitudes,

$$y_n'(\tau) + i\Omega_c y_n(\tau) = \left[g(1 - \omega_n^2) - 1 - i\beta\omega_n^2\right]y_n$$
$$+ (1 + i\gamma)\sum_{k-l+m=n} y_k y_l^* y_m,$$

(9)

and Taylor expand the gain,

$$g = \frac{a_c^2(1 - a_c^2)}{|a_c + y_0|^2 + \sum_{k\neq 0}|y_k|^2} = (1 - a_c^2)$$

$$\times \left[1 + \sum_j \left(-\frac{2\operatorname{Re}y_0}{a_c} - \frac{|y_0|^2 + \sum_{k\neq 0}|y_k|^2}{a_c^2}\right)^j\right].$$
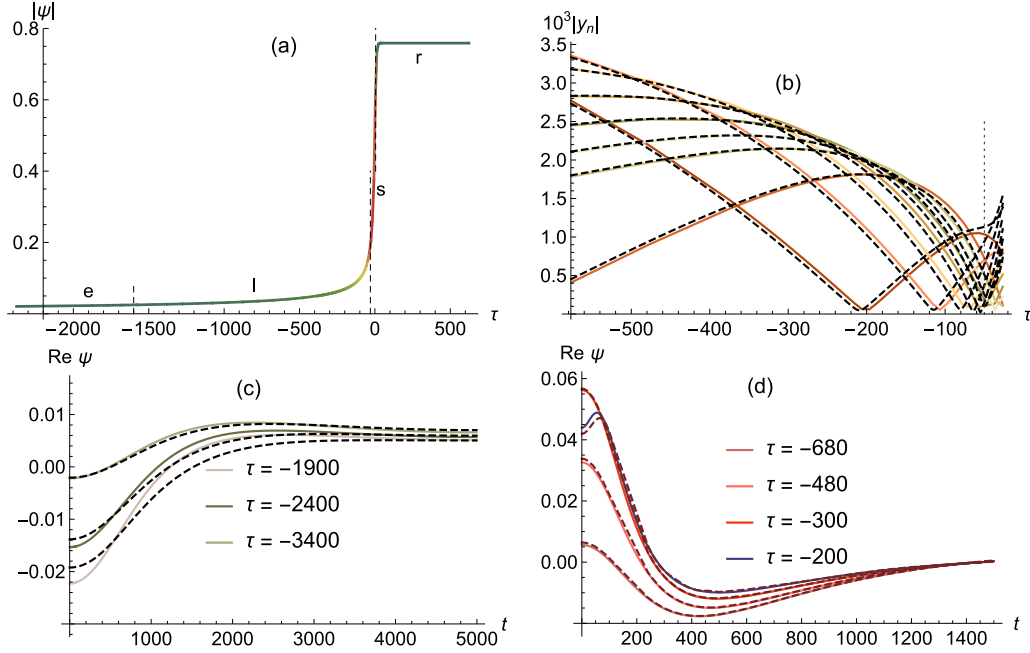
(10)

FIG. 3. Simulations and theory for pulse growth with $\beta = 0.5$, $\gamma = 2.0$, $k = 1.08$, $c = 0.34$. See Fig. 1 for panel descriptions.

As the pulse wave form is an even function, we will assume for simplicity that ψ is an even function of t initially, and therefore for all τ, so that $y_{-n}(\tau) = y_n(\tau)$.

Since y_1 is the fastest growing mode, there is a time interval where it dominates all higher modes, while still being a small perturbation of the cw amplitude,

$$a_c \gg |y_1(\tau)| \gg |y_n(\tau)|, \quad n \geqslant 2. \tag{11}$$

For such τ values y_1 grows according to the linearized dynamics Eq. (6), so that

$$y_1(\tau) = \alpha_1(1 + i\gamma)e^{\lambda\tau}, \quad \lambda = 2a_c^2, \quad \alpha_1 \text{ real} \tag{12}$$

(neglecting ω_1^2 with respect to a_c^2).

Consider now (9) with $n = 2$. When (11) holds, the largest terms are those proportional to y_2, and the terms in the triple sum with $0 \leqslant k, -l, m \leqslant 1$. Neglecting all other nonlinearities, and using $\omega_2 \ll a_c$, the equation for y_2 becomes

$$y_2'(\tau) = (1 + i\gamma)a_c^2(y_2 + y_2^*)$$
$$+ (1 + i\gamma)[2(1 + \gamma^2) + (1 + i\gamma)^2]a_c\alpha_1^2 e^{2\lambda\tau}, \tag{13}$$

using (12). Since the nonlinear growth rate in this equation, 2λ, is faster than λ_2, the linear growth rate of y_2, it eventually dominates the dynamics, so that for large τ,

$$y_2(\tau) = \frac{\alpha_1^2}{2a_c}(1 + i\gamma)(3 + i\gamma)e^{2\lambda\tau} \equiv \alpha_2(1 + i\gamma)e^{2\lambda\tau}. \tag{14}$$

Proceeding in the same fashion for higher n, we find

$$y_n(\tau) \sim \alpha_n(1 + i\gamma)e^{n\lambda\tau} - \delta_{n,0}a_c, \tag{15}$$

$$\alpha_n = \frac{(3 + i\gamma)\cdots(2n - 1 + i\gamma)}{n!}\frac{\alpha_1^n}{a_c^{n-1}}, \quad n \geqslant 0, \tag{16}$$

with the convention $\alpha_0 = a_c$.

Our next goal is to calculate the wave form $\psi(t, \tau)$. It is not sufficient for this purpose to sum the leading term for each

mode, since subleading terms in y_n can be as large or larger than the leading term in y_m, $m > n$. We therefore look for solutions of the form

$$y_n(\tau) = \sum_{\nu=0}^{\infty} \alpha_{n,\nu}(1 + i\gamma)e^{(n+2\nu)\lambda\tau} - \delta_{n,0}a_c, \tag{17}$$

where $\alpha_{n,0} = \alpha_n$ of Eq. (15). Plugging this expansion in (9) yields a system of equations for the coefficients where $\alpha_{n,\nu}$ is determined by $\alpha_{n+1,\nu-1}, \ldots, \alpha_{n+\nu,0}$, which can be solved recursively. The results of this calculation are in excellent agreement with direct simulations, as shown in Figs. 1(b), 2(b) and 3(b).

In the early stage of pulse growth, the bandwidth is small, and terms proportional to ω_n^2 are negligible in (9). Although we could not find a closed-form expression for the coefficients $\alpha_{n,\nu}$, we verified order by order that, when gain bandwidth and dispersion are neglected, the coefficients $\alpha_{n,\nu}$ are such that (15) *still holds*, up to an overall multiplicative factor, and moreover, the overall scale is such that the mean power remains *constant*,

$$\frac{1}{r}\int dt|\psi(t,\tau)|^2 dt = \sum_n |y_n(\tau)|^2 = a_c^2. \tag{18}$$

Summing the Fourier series defined by Eq. (17) then gives the early-stage wave form explicitly,

$$\psi_e(t,\tau) = a_w(t)\left[\left(1 - \frac{2\alpha_1(1 + i\gamma)}{a_c}e^{i\omega t + \lambda\tau}\right)^{-(1+i\gamma)/2}\right.$$
$$\left. + \left(1 - \frac{2\alpha_1(1 + i\gamma)}{a_c}e^{-i\omega t + \lambda\tau}\right)^{-(1+i\gamma)/2} - 1\right], \tag{19}$$

where

$$|a_w| = a_c \left[2F\left(\frac{1}{2}(1 - i\gamma), \frac{1}{2}(1 + i\gamma); 1; 4\frac{\alpha_1}{a_c} e^{2\lambda\tau} \right) - 1 \right]$$

(20)

is fixed by (18) (here F is the standard Gauss hypergeometric function.) This result is verified by comparison with simulations, in Figs. 1(c), 2(c) and 3(c).

The early growth wave form, where a fixed amount energy is squeezed in a decreasing time interval, becomes singular at τ_{sing}, defined by $2\alpha_1|1 + i\gamma|e^{\lambda\tau_{sing}} = a_c$. As the wave form approaches singularity, however, the bandwidth diverges, and effects of gain bandwidth and dispersion inevitably smoothen the pulse shape. Beyond this point, the full expansion (17) is needed for an accurate description of the waveform, as shown in Figs. 1(d), 2(d) and 3(d), and the pulse no longer has a simple invariant form. Interestingly, although gain filtering and dispersion check the growth of the pulse peak power, they cause the pulse energy to grow by an order-1 factor toward the final pulse energy.

Strongly nonlinear growth and relaxation. The expansion (17) has a finite radius of convergence, whose boundary is evident in the right edges of Figs. 1(b), 2(b) and 3(b). Beyond this point there is no small parameter, and the pulse dynamics becomes independent of the initial condition. This strongly nonlinear growth is much faster than the preceding dynamics, with the amplitude growing close to its final value in approximately 50 natural time units. Further study of the strongly nonlinear growth process and the relaxation to the final pulse wave form that follows it is beyond the scope of this work.

Conclusions. Saturable absorbers are a very effective means to produce strongly nonlinear ultrashort pulses, but the initial pulse growth they produce by modulational instability is very weak because the initial intensity contrasts are small. The weak initial growth can be inhibited by noise or by chaos, and it is what makes self-starting of passive mode locking hard.

Here, we study the growth of perturbations where the effects of noise and chaos are negligible. Although this assumption is strictly valid only for picosecond lasers, we conjecture that the mode cascade buildup mechanism discovered here also works in ultrashort lasers, once the initial barrier to self-starting has been crossed.

Since the linear growth rate is inversely proportional to the number of active modes, the duration of the growth process is mainly set by the time taken for the initial perturbation to grow to intensities that saturate the absorber. Nevertheless, the growth is not a linear process, except in its very early stage, when all mode amplitudes are comparable. Once the fastest growing mode dominates, it starts driving harmonics by four-wave mixing, making them grow much faster than the linear growth rate, so that the higher harmonics eventually catch up with the fundamental toward the creation of a short pulse.

Moreover, during most of the weakly nonlinear growth, each axial mode grows with a constant rate, except for an overall scale factor. As a consequence, the pulse maintains a fixed functional form and total energy, while narrowing and growing in amplitude. When the pulse amplitude reaches about 10% of the final amplitude, the dispersion and gain response break the form invariance; at this stage the full weakly nonlinear asymptotic series is necessary and sufficient for a good approximation of the wave form.

When the pulse amplitude further grows to about 30% of its final value, the weakly nonlinear perturbation series ceases to converge altogether, and the growth transitions to the much faster strongly nonlinear stage. The last stage of pulse dynamics consists of relaxation toward the final stable shape and amplitude, and is characterized by a third time scale.

Numerical simulations confirm the theoretical analysis of the pulse growth for several values of weak-to-moderate Kerr and dispersion coefficients, that include both normal and anomalous dispersion. As expected, the weakly nonlinear analysis breaks down earlier when Kerr and dispersion are increased. The mode amplitude oscillations in Fig. 3(b) are an early sign of the complexity that is observed in ultrashort pulse lasers [21].

The mode cascade process has been demonstrated here for the most common case of a slow gain and fast absorber laser. Nevertheless, it likely explains the physical mechanism of absorptive instability growth in any passive mode-locked laser, including those with fast gain [29–31] and slow absorbers [32,33]. However, the details of the pulse evolution in the latter cases are different from those studied here, and are beyond the scope of the present work. More generally, four-wave mixing is a common source of modulational instabilities that lead to pulse formation, and although the mode cascade growth relies on some properties specific to lasers, it may be relevant for the growth of other types of dissipative solitons [34].

This work sheds light on the complex and sparsely studied process of pulse growth in nonlinear systems, with important implications to the starting of mode-locked lasers. It is likely that weakly nonlinear methods would facilitate a theory of the relaxation process. While the strongly nonlinear growth is by definition beyond the reach of perturbative analysis, it might be amenable to a resummation of the weakly nonlinear series developed here.

[1] H. A. Haus, IEEE J. Sel. Top. Quantum Electron. **6**, 1173 (2000).

[2] J. N. Kutz, SIAM Rev. **48**, 629 (2006).

[3] P. Grelu and N. Akhmediev, Nat. Photonics **6**, 84 (2012).

[4] S. K. Turitsyn, N. N. Rosanov, I. A. Yarutkina, A. E. Bednyakova, S. V. Fedorov, O. V. Shtyrina, and M. P. Fedoruk, Phys.-Usp. **59**, 642 (2016).

[5] F. Krausz, T. Brabec, and C. Spielmann, Opt. Lett. **16**, 235 (1991).

[6] H. A. Haus and E. P. Ippen, Opt. Lett. **16**, 1331 (1991).

[7] T. Brabec, C. Spielmann, and F. Krausz, Opt. Lett. **16**, 1961 (1991).

[8] J. C. Kuo, J. M. Shieh, C. D. Hwang, C. S. Chang, C. L. Pan, and K. H. Wu, Opt. Lett. **17**, 334 (1992).

[9] N. Sarukura and Y. Ishida, Opt. Lett. **17**, 61 (1992).

[10] G. Cerullo, S. Desilvestri, and V. Magni, Opt. Lett. **19**, 1040 (1994).

[11] N. W. Pu, J. M. Shieh, L. Lai, and C. L. Pan, Opt. Lett. **20**, 163 (1995).

[12] D. H. Sutter, I. D. Jung, F. X. Kärtner, N. Matuschek, F. Morier-Genoud, V. Scheuer, M. Tilsch, T. Tschudi, and U. Keller, IEEE J. Sel. Top. Quantum Electron. **4**, 169 (1998).

[13] J. H. Sun, R. B. Zhang, Q. Y. Wang, L. Chai, D. Q. Pang, J. M. Dai, Z. G. Zhang, K. Torizuka, T. Nakagawa, and T. Sugaya, Appl. Opt. **40**, 3539 (2001).

[14] A. Gordon and B. Fischer, Phys. Rev. Lett. **89**, 103901 (2002).

[15] O. Gat, A. Gordon, and B. Fischer, Phys. Rev. E **70**, 046108 (2004).

[16] B. Vodonos, A. Bekker, V. Smulakovsky, A. Gordon, O. Gat, N. K. Berger, and B. Fischer, Opt. Lett. **30**, 2787 (2005).

[17] O. Gat, A. Gordon, and B. Fischer, New J. Phys. **7**, 151 (2005).

[18] A. Gordon, O. Gat, B. Fischer, and F. X. Kärtner, Opt. Express **14**, 11142 (2006).

[19] H. Li, D. G. Ouzounov, and F. W. Wise, Opt. Lett. **35**, 2403 (2010).

[20] L. Zinkiewicz, F. Ozimek, and P. Wasylczyk, Laser Phys. Lett. **10** 125003 (2013).

[21] G. Herink, B. Jalali, C. Ropers, and D. R. Solli, Nat. Photonics **10**, 321 (2016).

[22] P. Ryczkowski, M. Närhi, C. Billet, J.-M. Merolla, G. Genty, and J. M. Dudley, arXiv:1706.08571 [physics.optics].

[23] S. Wang, A. Docherty, B. S. Marks, and C. R. Menyuk, J. Opt. Soc. Am. B **31**, 2914 (2014).

[24] N. G. Usechak and G. P. Agrawal, Opt. Express **13**, 2075 (2005).

[25] N. G. Usechak and G. P. Agrawal, J. Opt. Soc. Am. B **22**, 2570 (2005).

[26] B. G. Bale and J. N. Kutz, J. Opt. Soc. Am. B **25**, 1193 (2008).

[27] C. J. Chen, P. K. A. Wai, and C. R. Menyuk, Opt. Lett. **19**, 198 (1994).

[28] T. Kapitula, J. N. Kutz, and B. Sandstede, J. Opt. Soc. Am. B **19**, 740 (2002).

[29] R. Paiella, F. Capasso, C. Gmachl, D. L. Sivco, J. N. Baillargeon, A. L. Hutchinson, A. Y. Cho, and H. C. Liu, Science **290**, 1739 (2000).

[30] M. Marconi, J. Javaloyes, S. Balle, and M. Giudici, Phys. Rev. Lett. **112**, 223901 (2014).

[31] J. Javaloyes, P. Camelin, M. Marconi, and M. Giudici, Phys. Rev. Lett. **116**, 133901 (2016).

[32] F. X. Kärtner, I. D. Jung, and U. Keller, IEEE J. Sel. Top. Quantum Electron. **2**, 540 (1996).

[33] C. R. Menyuk and S. Wang, Nanophotonics **5**, 332 (2016).

[34] N. Akhmediev and A. Ankiewicz, *Dissipative Solitons* (Springer, Berlin, 2005).